ELSEVIER Science Press
Trans. Nonferrous Met. Soc. China 19(2009) s183−s188
Transactions of Nonferrous Metals Society of China
www.tnmsc.cn

Measurement of metal vapor cooling speed during nanoparticle formation by pulsed wire discharge

Yuu SHIKODA[1], Yoshinori TOKOI[2], Koji SUWA[1], Satoru ISHIHARA[3], Tsuneo SUZUKI[1], Tadachika NAKAYAMA[1], Hisayuki SUEMATSU[1], Koichi NIIHARA[1]

1. Extreme Energy-Density Research Institute, Nagaoka University of Technology, 1603-1 Kamitomiokamachi, Nagaoka, 940-2188, Japan;
2. Department of Electrical and Electronic Engineering, Niigata University, 2-8050 Ikarashi Nishiku, Niigata, 950-2181, Japan;
3. Inovertion Satellite Niigata, Japan Science and Technology Agency, NICO Techno-Praza 2F, 4-1-9 Shinsan, Nagaoka, 940-2127, Japan

Received 2 March 2009; accepted 30 May 2009

Abstract: Pulsed wire discharge(PWD) is one of nano-sized powder production methods. The object of this work is to study influence of the plasma/vapor/particle density using computer simulation and to establish temperature measurement method using a high-speed infrared thermometer in the PWD process. The temperature correction coefficient was obtained from geometric computer simulation results. Obtained correction coefficient was applied to the temperature measuring results. It was found from this result that obtained correction coefficient was appropriate. A temperature measurement method was established by using the high-speed infrared thermometer in PWD.

Key words: pulsed wire discharge; nano-sized powder; infrared thermometer

1 Introduction

Pulsed wire discharge(PWD) is one of gas-phase process nano-sized powder production methods[1−4]. This method is characterized by several advantages. For example, this method can prepare different nano-sized powders of metals or compounds in a small chamber, and the energy efficient for particle production is very high [4−6]. The process for preparation of nano-sized powders using this method is as follows. Metal wire is rapidly heated by a pulsed current, and turns into vapor and plasma. Then, the vapor and plasma are rapidly cooled by the ambient gas to liquidify and solidify. Finally, nano-sized powder is formed. In the previous research, various process models of PWD such as a heating model of wire, a growth model of particle, and a droplet formation mechanism have been suggested[7−8]. However, the mechanism clarification is not completed because PWD formed particles in very short time.

One of the non-clarified processes is control of crystalline phase of the synthesized particles. For example, metallic oxides such as Al_2O_3, TiO_2 and ZrO_2 are known to have polymorphism. These particles were confirmed to be synthesized on PWD, but some phases could not be obtained[4, 9−10]. The reason has been considered that the phase depends on the cooling speed of vapor, liquid or solidification. To confirm this assumption, we think that measuring the temperature of particles using a high-speed infrared thermometer can yield some knowledge.

There is a problem in the measurement of temperature in PWD, that is, the high-speed infrared thermometer senses energy of photons with a certain wavelength from a limited volume, and measured temperature decreases with decreasing the plasma/vapor/particle density[11]. Thus, the object of this work is to study influence of the plasma/vapor/particle density using computer simulation and to establish a temperature measurement method using the infrared thermometer by

Corresponding author: Yuu SHIKODA; E-mail: shikoda@etigo.nagaokaut.ac.jp

PWD.

2 Simulation and experiment methods

2.1 Simulation

Schematic diagrams of temperature measured area by the infrared thermometer are illustrated in Fig.1. Some particles overlap if this area is seen from the infrared thermometer direction. Therefore, if the measured area has sufficient particle number density, measured area will be equivalent to a bulk body, which can yield accurate temperature data from the infrared thermometer. If the particle number density is lowered, there will be pores in the measured area. The total energy of photons to the infrared thermometer is decreased, and the measured temperature becomes lower than that of the actual temperature of particles. In this work, a geometric computer simulation was used by assuming that produced particles are not agglomerated and uniformly distributed.

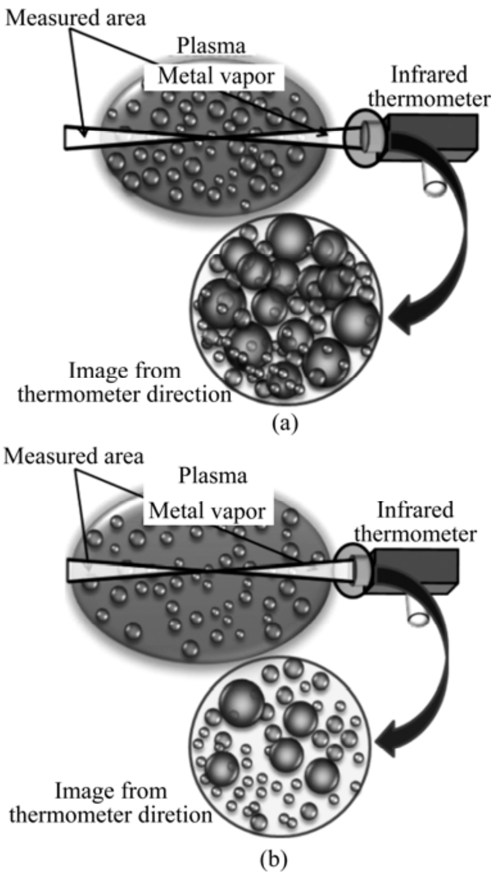

Fig.1 Schematic diagrams of particle distributions with higher number density (a) and lower number density (b) in temperature measured area by high-speed infrared thermometer

Fig.2 and Table 1 show a mesh and conditions for the simulation, respectively. In the simulation, x and y of temperature measured area of 0.1 mm×0.1 mm were divided into 4×10^8 pieces of 5 nm×5 nm. For x and y coordinates of a particle with size of 25 nm×25 nm, the random values were generated using Mersenne Twister algorithm. Then, the particle was placed on a cell with the x and y coordinates so that adjacent 25 cells were pasted. This process was repeated to the number of particles decided by calculating from plasma or vapor volume, metal wire volume, and particle volume.

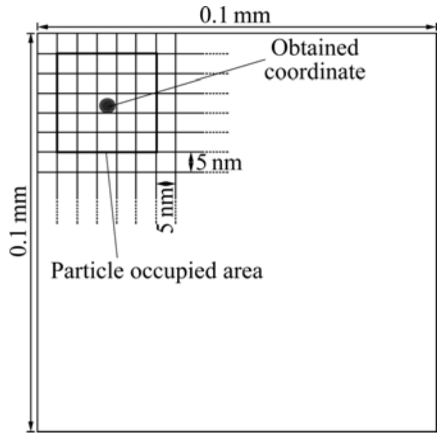

Fig.2 Schematic diagram of mesh used in simulation

This simulation code was programmed by C language. Particle occupied ratio of temperature measurement direction of the infrared thermometer (ρ) was defined as areal pasted ratio of the mesh.

2.2 Temperature measurement of PWD by infrared thermometer

Fig.3 shows a schematic diagram of the experimental set-up for PWD. The capacitor was charged using a high voltage power supply. The wire located in an ambient gas was exploded by closing a spark gap switch. The prepared powders in the chamber were evacuated with ambient gas by a rotary pomp. Prepared powders were collected on a membrane filter located midway between the chamber and the rotary pomp.

At the same time, light of the spark gap switch was detected by a photo detector and the signal was input to trigger the infrared thermometer. This started the temperature measurement. Temperature measured area was at the center of the electrode with area of about ϕ 1 mm. Specification of using the infrared thermometer

Table 1 Simulation conditions for estimating ρ in PWD process

Measured area	Number of division in x-direction	Number of division in y-direction	Plasma or vapor expand diameter/mm	Wire	
				Diameter/mm	Length/mm
0.1 mm×0.1 mm	20 000	20 000	25, 50, 75, 100, 150, 200, 250, 300	0.1, 0.2, 0.3	25

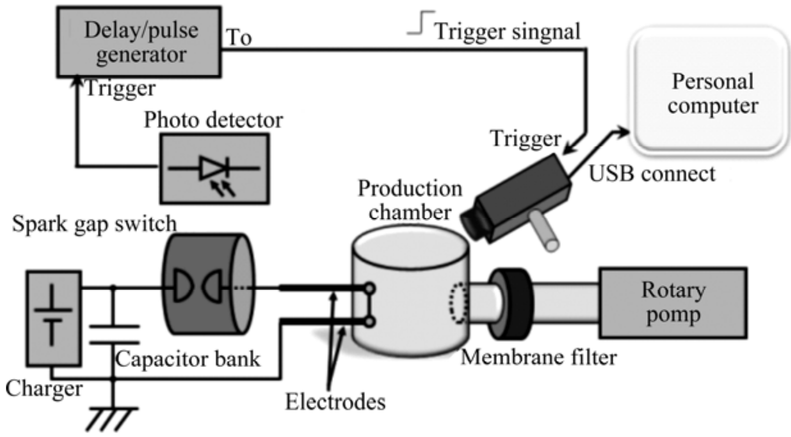

Fig.3 Schematic diagram of experimental set-up for synthesis of Cu particles by PWD

is shown in Table 2. Framing photographs of the expanding plasma/vapor/particle were taken by a high-speed camera.

Table 2 Specification of high-speed infrared thermometer

Measured temperature/℃	Spectral range/mm	Response time/μs	Measured field
350−3 500	2.0−2.5	10	About ϕ 1 mm

In these experiments, the voltage between the electrodes and the current of the discharge circuit was measured with a digitized oscilloscope using two high voltage probes and a current transfer during the discharge.

The experimental conditions are listed in Table 3. Nitrogen pressure was varied in the range of 10−100 kPa. The vaporization energy of copper wire with 0.1 mm in diameter and 25 mm in length was calculated to be 10.8 J.

Table 3 Experimental conditions of Cu particles prepared by PWD

Wire	Vaporization energy/J	Capacitor/μF	Charging voltage/kV
Cu ϕ 0.1 mm×25 mm	10.8	30	6
Charging energy/J	Ambient gas	Gas pressure/kPa	
540	N_2	10, 50, 100	

3 Results and discussion

3.1 Simulation result

The simulation results are shown in Fig.4. Measured temperature should be accurate from this simulation results to plasma/vapor/particle expanding diameter of 50, 100 and 150 mm for wire diameter of 0.1, 0.2 and 0.3 mm, respectively. Above these diameters, obtained temperature values must be corrected using ρ. Fig.5 shows the relationship between plasma/vapor/particle expanding diameter and particle occupied ratio of temperature measured direction, calculated from Fig.5. It was found from the simulation result that particle occupied ratio of temperature measured direction decreased drastically when plasma/vapor/particle expanding diameter became 150 mm for 0.3 mm in wire

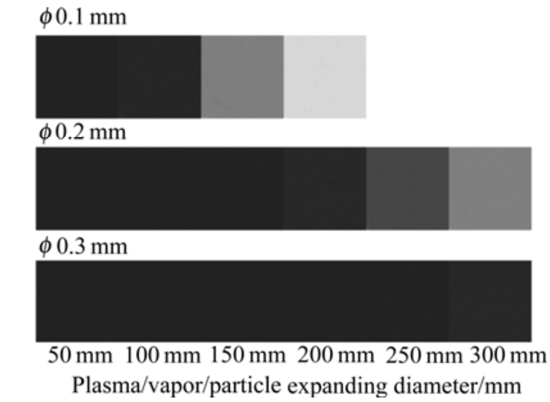

Fig.4 Distribution of particles obtained by simulation

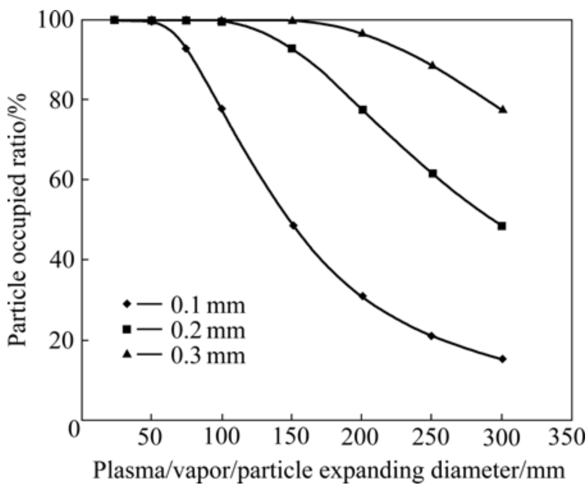

Fig.5 Simulation results of relationship between plasma/vapor/ expanding diameter and particle occupied ratio

diameter, over 100 mm for 0.2 mm in wire diameter, and 50 mm for 0.1 mm in wire diameter.

The simulation results were fitted by polynomial approximation of least square. The following shows the formula to calculate temperature correction coefficient(k) from measured temperature(T_m) to estimated temperature (T_e) in plasma/vapor/particle expanding diameter from fitted result:

$$T_e=kT_m \tag{1}$$

$$k=1+\left(1-\frac{Ad^5+Bd+Cd+Dd^2+Ed+F}{100}\right) \tag{2}$$

where d is plasma/vapor/particle expanding diameter. $A-F$ values are shown in Table 4.

3.2 Temperature measurement of PWD by infrared thermometer

Figs.6 and 7 show such voltage/current waveforms and framing photographs of the expanding plasma in explosion of copper wire. It was found that the current became zero at about 70 μs, which was the end point of the heating. From this result, the temperature correction coefficient(k) was calculated using d obtained from the framing photographs of Fig.7 of the expanding plasma at

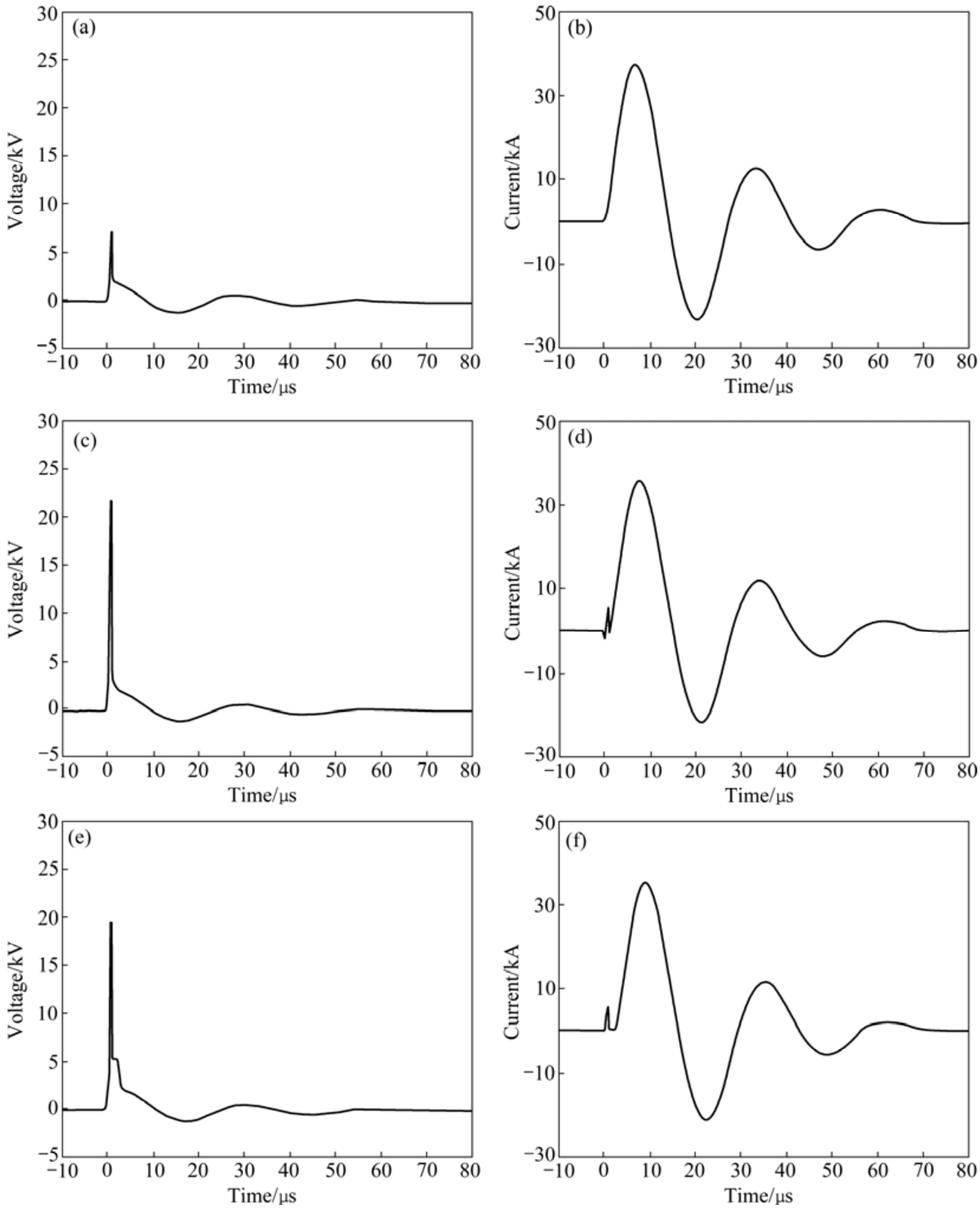

Fig.6 Voltage/current waveforms of discharging Cu wire of ϕ 0.1 mm×25 mm in N_2 at 10 kPa (a) and (b), 50 kPa (c) and (d) and 100 kPa (e) and (f)

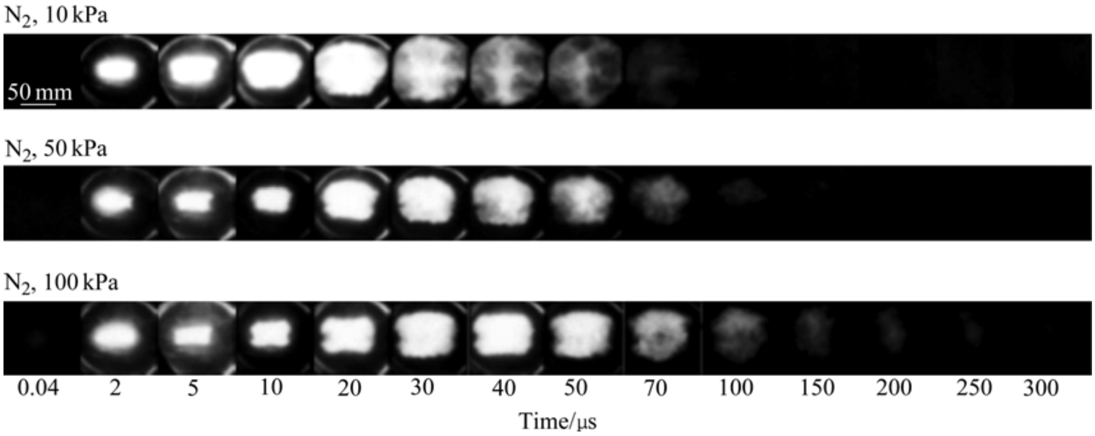

Fig.7 Framing photographs of expanding plasma of Cu wire

Table 4 Fitted coefficients to calculate *k*

Coefficient	ϕ 0.1 mm	ϕ 0.2 mm	ϕ 0.3 mm
A	2.198×10^{-10}	-1.794×10^{-10}	9.774×10^{-11}
B	2.654×10^{-7}	1.729×10^{-7}	6.910×10^{-8}
C	1.170×10^{-4}	5.714×10^{-5}	1.513×10^{-5}
D	2.204×10^{-2}	6.827×10^{-3}	1.37×10^{-3}
E	1.251	0.310 8	5.15×10^{-2}
F	80.46	104.4	99.36

70 μs. Plasma/vapor/particle expanding diameter was calculated by the method that emission intensity of the flaming photograph along the kitty-cornered direction was analyzed using an image processing software. Fig.8 shows result of emission intensity of the framing photographs at 70 μs. The measured plasma/vapor/particle expanding diameter from Fig.8 and fitted the temperature correction coefficients are listed in Table 5.

Fig.9 shows temperature measurement results by infrared thermometer before and after temperature correction. It was found from the Fig.9(a) that cooling

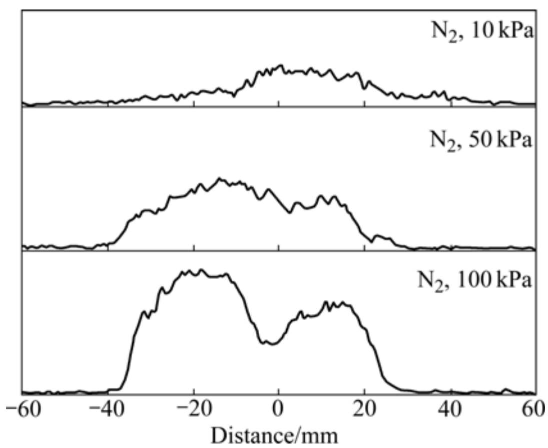

Fig.8 Results of analyzed emission intensity of flaming photographs

Table 5 Analyzed results of plasma/vapor diameter and calculation results of temperature correction coefficient

Gas pressure/kPa	Expanding diameter/mm	Temperature correction coefficient (*k*)
10	110.0	1.28
50	84.4	1.13
100	78.9	1.10

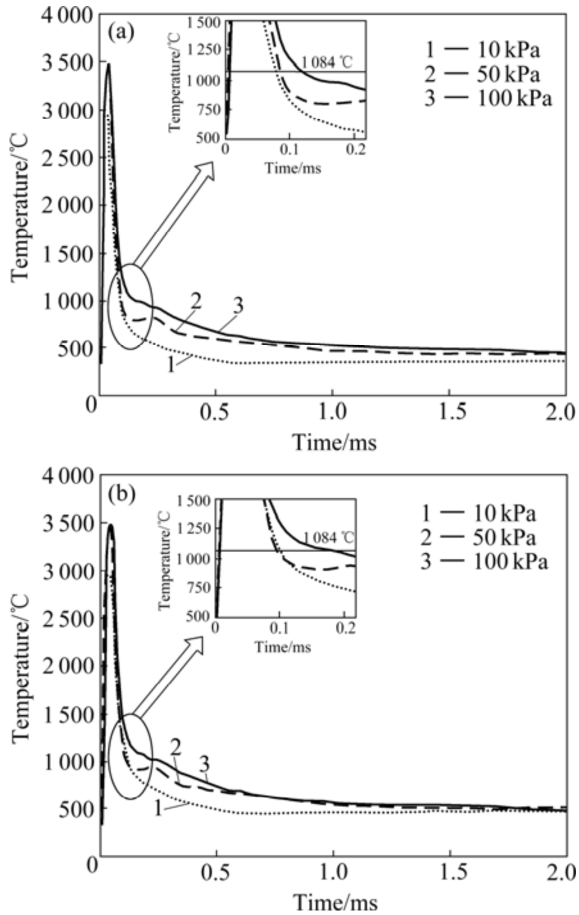

Fig.9 Time evolution of temperature measurement before temperature correction (a) and after temperature correction (b)

speed slowered drastically after t=0.1 ms. The cause was considered that thermal dissipation was retarded to form the solid particles by the latent heat. Thus, the point of cooling speed slowing down should correspond to the melting point of copper (1 084 ℃).

By comparing Figs.9(a) and (b), the temperatures of cooling speed slowing down coincided comparatively better with melting point of copper in that after-correction. These results lead to the conclusion that simulation result and obtained temperature correction coefficient are appropriate.

4 Conclusions

1) The accuracy of temperature correction coefficient was estimated from geometric computer simulation results.

2) Obtained correction coefficient was applied to temperature measurement results. It was found from this result that obtained correction coefficient was appropriate.

3) The metal vapor cooling speed by PWD is measureable.

Acknowledgement

This work was supported by Science and Technology Agency of Japan.

References

[1] FARADAY M. The bakerian lecture: Experimental relations of gold (and other metals) to light [J]. Philosphical Transactions of Royal Society of London, 1857, 147: 145−181.

[2] KOTOV Y A. Electric explosion of wires as a method for preparation of nanopowders [J]. Journal of Nanoparticle Research, 2003, 5: 539−550.

[3] UMAKOSHI M, YOSHITOMI T, KATO A. Preparation of alumina and alumina-silica powders by wire explosion resulting from electric discharge [J]. Journal of Materials Science, 1995, 30: 1240−1244.

[4] JIANG W, YATSUI K. Pulsed wire discharge for nanosize powder synthesis [J]. IEEE Transactions of Plasma Science, 1998 26: 1498−1501.

[5] NISHIMURA S, HAYASHI Y, SUZUKI T, NAKAMURA T, SUEMATSU H, JIANG W, YAMAZAKI A, SAKI K, NIIHARA K. Pulsed wire discharge apparatus for mass production of nanosized powders [J]. Advanced Materials Research, 2006, 11/12: 315−318.

[6] SUEMATSU H, NISHIMURA S, MURAI K, HAYASHI Y, SUZUKI T, NAKAYAMA T, JIANG W, YAMAZAKI A, SEKI K, NIIHARA K. Pulsed wire discharge apparatus for mass production of copper nanopowders [J]. Review of Scientific Instruments, 2007, 78: 056105.

[7] CHO C, MURAI K, SUZUKI T, SUEMATSU H, JIANG W, YATSUI K. Enhancement of energy deposition in pulsed wire discharge for synthesis of nanosized powders [J]. IEEE Transactions of Plasma Science, 2004, 32: 2062−2067.

[8] MURAI K, CHO C, SUEMATSU H, JIANG W, YATSUI K. Particle size distribution of copper nanosized powders prepared by pulsed wire discharge [J]. IEEJ Transactions of Fundamental Materials, 2005, 125: 39−44.

[9] SUZUKI T, KEAWCHAI K, JIANG W, YATSUI K. Nanosize Al_2O_3 powder production by pulsed wire discharge [J]. Japanese Journal of Applied Physics, 2001, 40: 1073−1075.

[10] TOKOI Y, SUZUKI T, NAKAYAMA T, SUEMATSU H, JIANG W, NIIHARA K. Synthesis of TiO_2 nanosized powder by pulsed wire discharge [J]. Japanese Journal of Applied Physics, 2008, 47: 760−763.

[11] Japan Electric Measuring Instruments Manufacturers' Association. Proper method for using thermometer [M]. Tokyo: Japan Industrial Publishing, 2007: 186. (in Japanese)

(Edited by YANG Hua)